BL Practice: BL08W, *Cheiron2008*

Fermi Surface and Electron Correlation Effects Probed by Compton Scattering

Yoshiharu Sakurai
Japan Synchrotron Radiation Research Institute

1. Introduction to Compton scattering [1]

Most of physics students remember having learned the Compton effect, i.e. the effect of Compton scattering, from an introductory lecture or textbook on quantum ideas. The Compton effect, the increase in the wavelength, i.e. the decrease in the energy, of X-rays or gamma-rays on being scattered by material objects, obviously demonstrates that X-rays and gamma-rays have a particle nature and these particles, the photons, behave like materials particles in collision with electrons in material objects.

Considering a collision between a photon and an electron, the conservation laws for energy and momentum lead to a simple result for the energy shift (ΔE) of the photon by Compton scattering,

$$\Delta\mathrm{E}=\frac{\hbar^2\mathbf{q}^2}{2m}+\frac{\hbar\mathbf{q}\cdot\mathbf{p}}{m}, \qquad (1)$$

where $\mathbf{p}=(p_x,p_y.p_z)$ is the electron momentum before scattering, **q** the scattering vector, m the electron mass. The first term is the fixed shift in energy only depending on the scattering geometry, and the second one is a Doppler shift that depends on the component of the electron momentum along the scattering vector **q**.

Summing up all events of Compton scattering with moving electrons in a material object, the Compton-scattered X-ray line appears as a broadening one (see Fig.1), and the line shape is converted into the so-called Compton profile, $J(p_z)$, under the impulse approximation,

$$\mathrm{J}(\mathrm{p_z}) = \iint \mathrm{n}(\mathbf{p})\mathrm{dp_x dp_y}, \qquad (2)$$

where n(**p**) is the electron momentum density, the probability distribution of the electron momenta, in a material object, and the z direction is taken along the scattering vector **q**. The Compton profile can be normalized to the total number of electrons N in the material object,

$$\int \mathrm{J}(\mathrm{p_z})\mathrm{dp_z} = \mathrm{N}. \qquad (3)$$

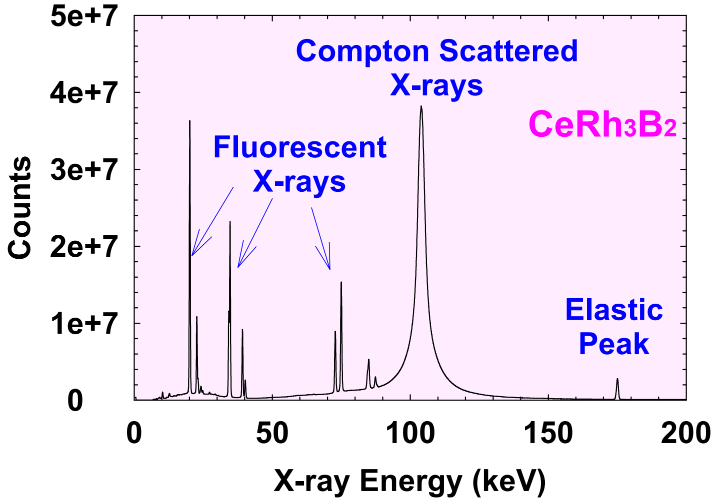

Fig.1: X-ray energy spectrum from $CeRh_3B_2$ measured by a Ge solid state detector with a scattering angle of 168 degrees. The incident X-ray energy is 175 keV at the Elastic Peak and the Compton Scattered X-rays line at 105 keV is broadened by the Doppler shift in collision between photons and moving electrons.

2. Fermi surface and electron correlation effects by Compton scattering

The defining property of a metallic ground state is the “Fermi surface,” which marks the boundary the electron occupied and unoccupied states in momentum space (see Fig.2), and thus the electron momentum density, $n(\mathbf{p})$, reflects the shape of Fermi surfaces and delineates the electron correlation effects in momentum space. The Compton profile contains the signatures of underlying Fermi surfaces, since it is given as a double integration of $n(\mathbf{p})$ (see eq.(2)) [2].

In order to map out the Fermi surface, one need to know the three-dimensional momentum density, $n(\mathbf{p})$, or two-dimensional one, $n(p_x, p_y) = \int n(\mathbf{p})dp_z$. In the Compton experiment, one can obtain the three- or two-dimensional momentum density using a topographic reconstruction from experimental $J(p_z)$’s measured along different crystal directions.

The advantage of Compton scattering over other probes for Fermiology are that it do not need a nearly lattice-defect-free crystal or clean surface or ultra high vacuum or very low temperature. For example, one can map out the Fermi surface of a disordered alloy in gas atmosphere at room temperature. Even with these advantages Compton scattering had not been a workable probe for more than half a century, because the method requires high energy (~100 keV) photons with high flux ($\sim 1\times10^{13}$ photons/s) that can be available only at large-scale synchrotron radiation facilities such as SPring-8 and ESRF. Fermiology by high-resolution Compton scattering has now been developed to such that it can now provide information about Fermi surface of various materials [3-7].

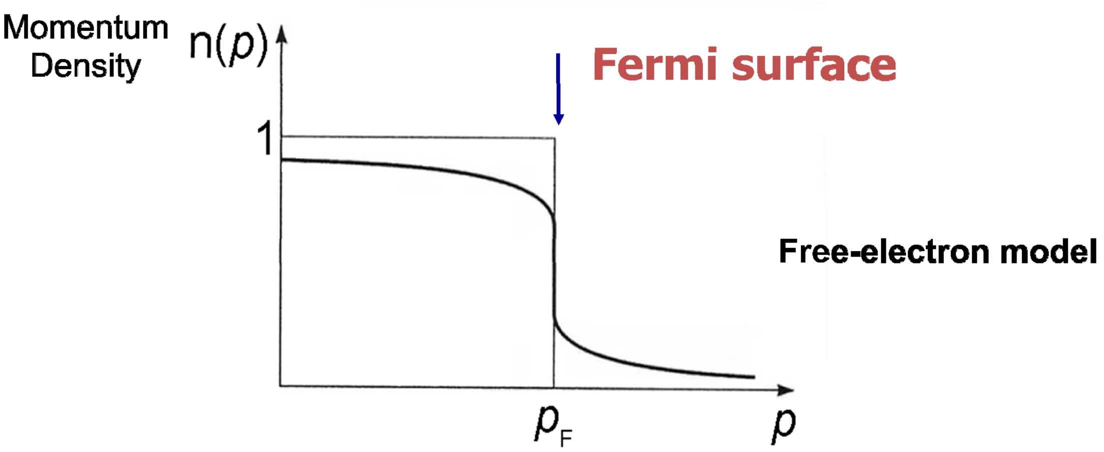

Fig.2: The Fermi surface is defined as a boundary between electron occupied and unoccupied states in momentum space. The thin line shows the electron momentum density of the free electron model, in which a step-like discontinuity appears at the Fermi surface in the momentum density profile. When the interaction between electrons is turned on (interacting electrons), some of the weights in the density are moved from $p < p_F$ to $p > p_F$, although the discontinuity remains at the Fermi surface. The difference in n(p) between the free and interacting electrons shows the electron correlation effects on the electron momentum density.

3. An examples of Fermi surface mapping: Ni_xAl_{1-x} (x=0.625) [4]

The Fermi surface of the shape-memory alloy $Ni_{0.62}Al_{0.38}$ was determined using the Compton scattering technique. A large area of this Fermi surface can be made to nest with other areas by translation through a vector of $\approx 0.18[1,1,0](2\pi/a)$, which corresponds to the wave vector associated with martensitic precursor phenomena such as phonon softening and diffuse streaking in electron diffraction patterns. This results provides a piece of evidence that these phenomena are driven by the enhanced electron-lattice coupling due to the Fermi surface nesting

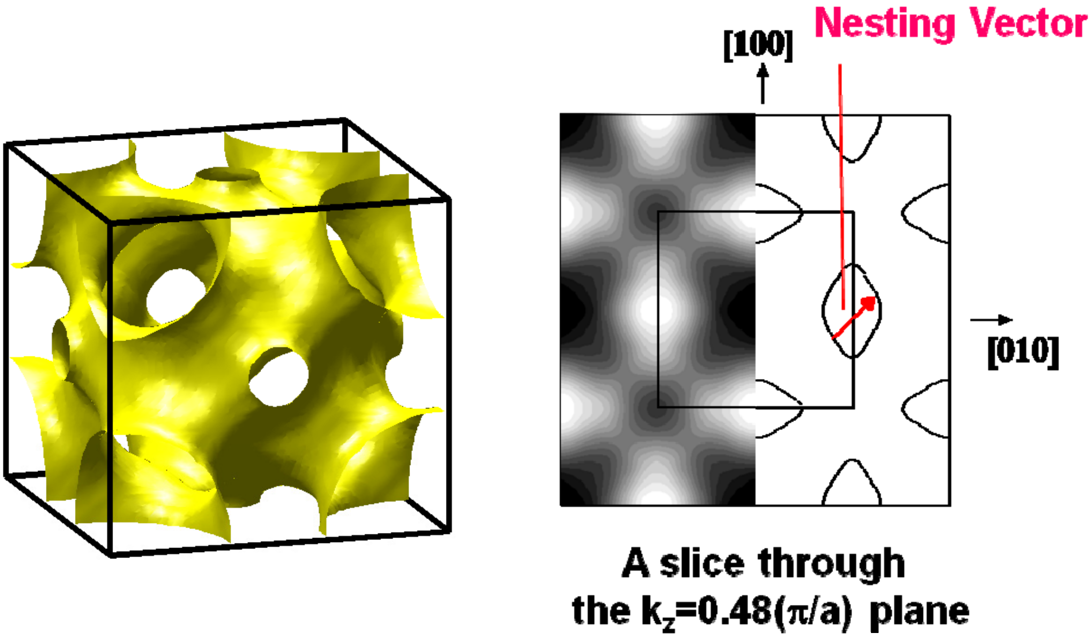

Fig.3: Fermi surface and its nesting feature in $Ni_{0.62}Al_{0.38}$ determined by Compton scattering.

4. Practice

In this beamline practice, we measure the Compton profiles of Al and V. Al is a simple metal with a Fermi surface of nearly free electron, whose shape is a sphere in an extended zone. V is a 3d metal with complicated Fermi surfaces because of large contribution of 3d electrons to the Fermi surfaces.

The aim of this practice is to learn the X-ray spectrometer [8-10] (see Fig.4) for Compton scattering experiment and to find the difference in Compton profiles between the nearly free electron and complicated 3d electron Fermi surfaces.

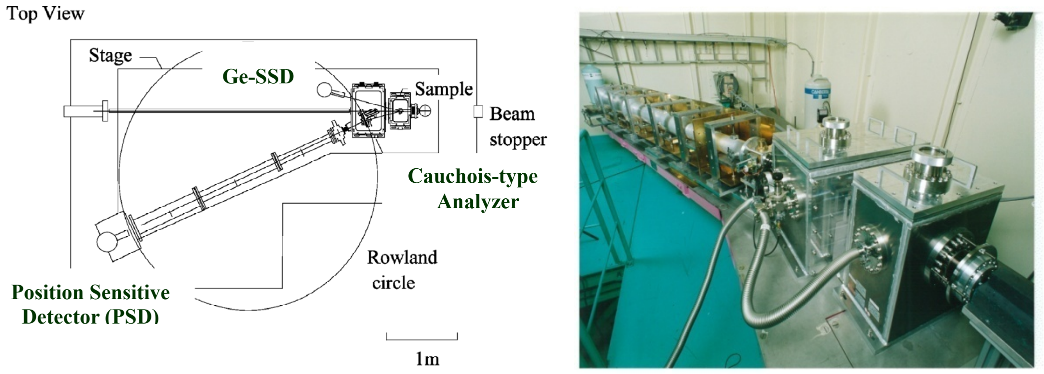

Fig.4: X-ray spectrometer for Compton scattering experiments at BL08W.

References

[1] See, e.g., M. J. Cooper, Rep. Prog. Phys. **48, 415** (1985).
[2] Y. Sakurai, Y. Tanaka, A. Bansil, S. Kaprzyk, A. T. Stewart, Y. Nagashima, T. Hyodo, S. Nanao, H. Kawata, and N. Shiotani, Phys. Rev. Lett. **74**, 2252 (1995).
[3] S. Mizusaki, T. Miyatake, N. Sato, I. Yamamoto, M. Yamaguchi, M. Itou, and Y. Sakurai , Phys. Rev. B **73**, 113101 (2006).
[4] S. B. Dugdale, R. J. Watts, J. Laverock, Zs. Major, M. A. Alam, M. Samsel-Czekala, G. Kontrym-Sznajd, Y. Sakurai, M. Itou, and D. Fort, Phys. Rev. Lett. **96**, 046406 (2006).
[5] N. Hiraoka, T. Buslaps, V. Honkimäki, J. Ahmad, and H. Uwe, Phys. Rev. B **75**, 121101(R) (2007).
[6] N. Hiraoka, T. Buslaps, V. Honkimäki, T. Nomura, M. Itou, Y. Sakurai, Z. Q. Mao, and Y. Maeno, Phys. Rev. B **74**, 100501(R) (2006).
[7] J. Laverock, S. B. Dugdale, J. A. Duffy, J. Wooldridge, G. Balakrishnan, M. R. Lees, G. –q. Zheng, D. Chen, C. T. Lin, A. Andrekczuk, M. Itou, and Y. Sakurai, Phys. Rev. B **76**, 052509 (2007).
[8] N. Hiraoka, M. Itou, T. Ohata, M. Mizumaki, Y. Sakurai and N. Sakai, J. Synchrotron Rad. **8**, 26 (2001).
[9] M. Itou and Y. Sakurai, AIP Conference Proceedings, **705**, 901 (2004).
[10] Y. Sakurai and M. Itou, J. Phys. Chem. Solids, **65**, 2061 (2004).